Multifaceted role of the complement system in health and disease: a focus on properdin

Essen, M.F. van

Initial properdin binding contributes to alternative pathway activation at the surface of viable and necrotic cells

Mieke F. van Essen[1], Nicole Schlagwein[1], Elisa M.P. van den Hoven[1], Daniëlle J. van Gijlswijk-Janssen[1], Rosalie Lubbers[2], Ramon M. van den Bos[3], Jacob van den Born[4], Jurjen M. Ruben[1], Leendert A. Trouw[2,5], Cees van Kooten[1], on behalf of the COMBAT consortium

[1]Division of Nephrology and Transplant Medicine, Department of Medicine, Leiden University Medical Center, Leiden, The Netherlands.

[2]Department of Rheumatology, Leiden University Medical Center, Leiden, The Netherlands.

[3]Faculty of Science, Department of Chemistry, Crystal and Structural Chemistry, Bijvoet Center for Biomolecular Research, Utrecht University, Utrecht, The Netherlands.

[4]Department of Nephrology, University Medical Center Groningen, Groningen, The Netherlands.

[5]Department of Immunology, Leiden University Medical Center, Leiden, The Netherlands.

Eur J Immunol. 2022 Apr;52(4):597-608
doi: 10.1002/eji.202149259.

Abstract

Properdin, the only known positive regulator of the complement system, stabilizes the C3 convertase, thereby increasing its half-life. In contrast to most other complement factors, properdin is mainly produced extrahepatically by myeloid cells. Recent data suggest a role for properdin as a pattern recognition molecule. Here, we confirmed previous findings of properdin binding to different necrotic cells including Jurkat T cells. Binding can occur independent of C3, as demonstrated by HAP-1 C3 KO cells, excluding a role for endogenous C3. In view of the cellular source of properdin, interaction with myeloid cells was examined. Properdin bound to the surface of viable monocyte-derived pro- and anti-inflammatory macrophages, but not to DCs. Binding was demonstrated for purified properdin as well as fractionated P2, P3, and P4 properdin oligomers. Binding contributed to local complement activation as determined by C3 and C5b-9 deposition on the cell surfaces and seems a prerequisite for alternative pathway activation. Interaction of properdin with cell surfaces could be inhibited with the tick protein Salp20 and by different polysaccharides, depending on sulfation and chain length. These data identify properdin as a factor interacting with different cell surfaces, being either dead or alive, contributing to the local stimulation of complement activation.

Introduction

The complement system consists of three pathways, the classical (CP), lectin (LP) and alternative pathway (AP) and plays an important role in the defense against microorganisms and the removal of dead cells (reviewed in (1)). Properdin is the only known positive regulator of the AP, stabilizing the C3 convertase, increasing its half-life five to ten times (2). Properdin appears in dimers, trimers and tetramers (3). Recently, crystal structures of properdin provided new insights into the mechanism of C3 convertase stabilization (4,5).

There is also evidence that properdin is able to interact with surfaces directly, thereby contributing to complement activation (6). The exact mechanism of how properdin acts as a pattern recognition molecule (PRM) remains to be elucidated and is also still a matter of debate. Some investigations showed a need of initial C3b deposition prior to binding of properdin (7,8). Other studies have shown that properdin can interact directly with microbial surfaces, early and late apoptotic and necrotic cells, and proximal tubular epithelial cells (PTECs) (9–13). Our group recently showed properdin deposition in the glomeruli of C3 KO mice with induced acute antiglomerular basement membrane disease (14), providing evidence of a C3b-independent binding of properdin. The binding of properdin to tubular epithelial cells was shown to be mediated by heparan sulfates expressed on the cell surface (15–17).

Properdin, in contrast to other complement factors which are produced by the liver, is mainly produced by myeloid cells. Neutrophils contain a pool of properdin, both DCs and macrophages produce and secrete properdin (18–21). In addition, myeloid cells are able to produce and secrete other complement factors, contributing to local complement activation (22). In this study, we investigated the binding of properdin to different cell surfaces and not only confirmed binding to necrotic Jurkat T cells (11), but also observed binding to pro- and anti-inflammatory macrophages. Binding could be prevented by heparin, depending on the degree of sulfation, chain length and backbone composition of glycosaminoglycans (GAGs). Furthermore, Salp20, a tick protein from *Ixodes scapularis* (23,24) blocked properdin binding. Altogether, our data suggests that the binding of properdin to the cell surfaces is a prerequisite for AP activation on the cell surface.

Materials and methods

Cell culture

Necrotic Jurkat T cells were generated as described previously (Supporting information Fig. S1) (11). Monocytes were isolated and DCs were generated as described before (25). Pro- and anti-inflammatory macrophages were generated by supplementing monocyte-cultures with 10 ng/mL GM-CSF (premium grade, 130–093-868, Miltenyi Biotec) or 100 ng/mL M-CSF (premium grade, 130-096-493, Miltenyi Biotec), respectively. Analysis of differentiation is shown in the supporting information (Supporting information Fig. S3).

Protein production

Recombinant properdin and Salp20 were generated as described previously (5,26).

Fractionation of properdin

Purified properdin (~400µg, concentration 1 mg/ml, A412, lot 144323 and 181138, Quidel, San Diego, CA, USA), or a 3x concentrated sample, was loaded on a Superdex 200 Increase 10/300 (GE Healthcare) pre-equilibrated using PBS. Fractions were eluted with PBS at 0.5 or 0.25 mL/min and collected in 250 µL fractions. Fractions were pooled and properdin concentrations were determined by ELISA. Plates were coated (mouse monoclonal anti-human properdin, 0.3 µg/mL, A233, Quidel), blocked (PBS-1% BSA; Sigma-Aldrich, Saint Louis, MO, USA) and pooled fractions were measured in several dilutions (diluted in PBS containing 0.05% Tween 20 [Sigma-Aldrich]-1%BSA). Next, plates were washed with wash buffer (PBS containing 0.05% Tween 20) and incubated with rabbit anti human-properdin-digoxigenin (DIG; in-house, 1:2500) for 1 h at 37°C. After washing, plates were incubated with peroxidase-conjugated IgG fraction monoclonal mouse anti-DIG (0.1 µg/mL, 200-032-156, Jackson ImmunoResearch, Cambridgeshire, UK) for 1 h at 37°C and developed using 3,3',5,5'-tetramethylbenzidine (TMB, Sigma-Aldrich). The reaction was stopped using 1 M H_2SO_4. Absorbance was measured at 450 nm (iMark Microplate Reader, Bio-Rad, Hercules, CA, USA).

Properdin binding to cells

Purified properdin, either from Quidel (A412) or CompTech (A139, Tyler, TX, USA) was aliquoted and kept frozen (-80˚C). Recombinant produced properdin was stored at 4˚C. A total of 10 µg/mL properdin (Quidel; or otherwise indicated at the figure legends), was diluted in RPMI-1640 medium (no phenol red), followed by incubation with the cells for 1 h at 4˚C. Cells were washed and incubated with mouse-monoclonal anti-human properdin (2 µg/mL, A233, Quidel) for 30 min at 4˚C, followed by incubation with goat anti-mouse immunoglobulins/RPE, goat F(ab')2, RPE (5 µg/mL, R0480, DAKO, Santa Clara, CA, USA) for 30 min at 4˚C. Binding of oligomeric properdin structures P2, P3

and P4 was examined following a similar protocol. Binding was assessed using flow cytometry (LSR-II, BD).

Activation of classical (CP), lectin (LP) and alternative pathway (AP)

CP, LP and AP activity in normal human serum (NHS) was determined by ELISA (Supporting information Fig. S2).

C3 deposition on cell surfaces

Properdin binding, using either purified or oligomeric forms of properdin (Quidel), was performed as described above. Cells were washed and incubated (30 min, 37˚C) with 10% NHS either diluted in RPMI, RPMI-MgEGTA (RPMI-1640 containing 10 mM EGTA and 5 mM $MgCl_2$) or in RPMI-EDTA (RPMI-1640 containing 10 mM EDTA). Cells were washed and incubated (30 min, 4˚C) with mouse-anti human C3 (1/600, RFK22, in-house generated), followed by incubation with goat anti mouse – PE(F(ab')2 goat anti-mouse-IgG-RPE) (5 µg/mL, R0480, DAKO) diluted in RPMI (no phenol red, 30 min at 4˚C). C3 deposition was determined by flow cytometry (LSR-II, BD).

C5b-9 deposition on cell surfaces

Cells were blocked with pooled heat-inactivated NHS (ΔNHS, 10%) for 15 min at room temperature. Next, cells were washed and incubated with properdin (Quidel). Cells were washed and incubated with 10% NHS diluted in the described complement buffers (30 min, 37˚C). Cells were incubated with mouse monoclonal anti human C5b-9 (1 µg/mL, AE11, Hycult Biotech; 30 min, 4˚C) followed by incubation with goat anti mouse – PE(F(ab')2 goat anti-mouse-IgG-RPE) (5 µg/mL, R0480, DAKO), diluted in RPMI (no phenol red, 30 min at 4˚C). Deposition was determined by flow cytometry.

Serum as inhibitor

Properdin binding from NHS was examined by incubating necrotic Jurkat T cells with different percentages of NHS. Binding was examined as described above. In addition, properdin (10 µg/mL, Quidel) was incubated with various percentages of ΔNHS (twofold dilutions starting from 50%) for 30 min at 4˚C. Next, the mixture was added to necrotic Jurkat T cells and incubated for 1 h at 4˚C. Cells were washed and properdin binding was determined as described above. For C3 deposition, cells were washed with RPMI-MgEGTA and incubated with 10% properdin-depleted serum (A339, Comptech) for 30 min at 4˚C. Cells were washed and C3 deposition was determined by flow cytometry as described above.

Salp20 and properdin

A total of 10 µg/mL properdin (Quidel) was preincubated with various concentrations of Salp20 (30 min, 4˚C). Next, cells were incubated with the mixture (1 h, 4˚C). Properdin binding was analyzed by flow cytometry as described above. A FITC-labeled form of Salp20 was used to investigate the direct interaction of Salp20 with the cell surface.

The effect of Salp20 on properdin binding and AP activation was examined. Properdin and Salp20 (1000 nM) were preincubated and the mixture was added to necrotic Jurkat T cells. Cells were washed and incubated with 10% NHS diluted in RPMI-MgEGTA (30 min, 37˚C). C3 deposition was determined as described above.

Heparinoids and properdin

A total of 10 µg/mL purified properdin was preincubated with various concentrations of unfractionated heparin (LEO Pharma, Ballerup, Denmark), with either 0.1, 1 or 10 µg/mL *O*-sulfated and unsulfated K5 or with 10 µg/mL of polysaccharide derivatives: heparin, low molecular weight heparin, *O*-sulfated and unsulfated K5, fucoidan, dextran sulfate, unsulfated dextran T40, *N*-desulfated/reacetylated heparin, periodate oxidized/reduced heparin, chondroitin sulfate C, chondroitin sulfate B and heparin sulfate from bovine kidney (17). Mixtures were added to the cells (1 h, 4˚C). Properdin binding was detected by flow cytometry as described above.

Flow cytometric analysis

Acquired flow cytometric data was analyzed using FlowJo Software version 10.6.1 (Tree Star, Ashland, OR, USA). Cells were gated based on FSC-A versus SSC-A, followed by selection of single cells using FSC-A versus FSC-H, and examined for properdin-binding (Supporting information Fig. S1, S4A and B) or complement deposition, respecting the guidelines as described in Ref. (27).

Statistical analysis

Statistical analysis was performed by Wilcoxon matched-pairs signed rank test. Analysis between multiple groups was performed using a nonparametric one-way ANOVA (Friedman test with Dunn's multiple comparisons test). Significance was defined as $p \leq 0.05$. For statistical analysis and graphical representations GraphPad Prism v.9.0.1 was used (San Diego, CA, USA).

Results

Properdin binds to the surface of necrotic but not viable Jurkat T cells

To investigate the interaction of properdin with different cell surfaces, we incubated necrotic Jurkat T cells with properdin and used FACS analysis to show binding (Figure 1A and B, Supporting information Fig. S1A), confirming previous results (11). Properdin binding was dose-dependent (Figure 1C), and was observed with properdin derived from various sources, including serum-purified and recombinant properdin (Supporting information Fig. S1B). To exclude the contribution of nonphysiological aggregates, we fractionated properdin using size exclusion chromatography and peak fractions were pooled as indicated (Figure 1D). Incubation of viable Jurkat T cells with P2, P3 and P4 oligomers and unfractionated properdin did not result in binding, whereas binding was observed to necrotic Jurkat T cells (Figure 1E). The nonphysiological P > 4 form of properdin was able to bind to the surface of both viable and necrotic Jurkat T cells (Figure 1E). Binding capacity increased with increasing size, following a similar pattern as described before (28).

To exclude a contribution of endogenous C3 in facilitating properdin binding, we used C3 KO HAP-1 cells, generated using CRISPR-Cas9. Properdin bound weakly to the surface of viable HAP-1 cells, and very strongly to necrotic HAP-1 cells. Binding of purified properdin to WT HAP-1, HAP-1 control and C3 KO HAP-1 cells was comparable, indicating that properdin binding can occur independent from C3 (Figure 1F). Binding of properdin oligomers P2, P3 and P4 to C3 KO HAP-1 cells was also observed, with higher oligomeric structures showing increased binding (Figure 1G).

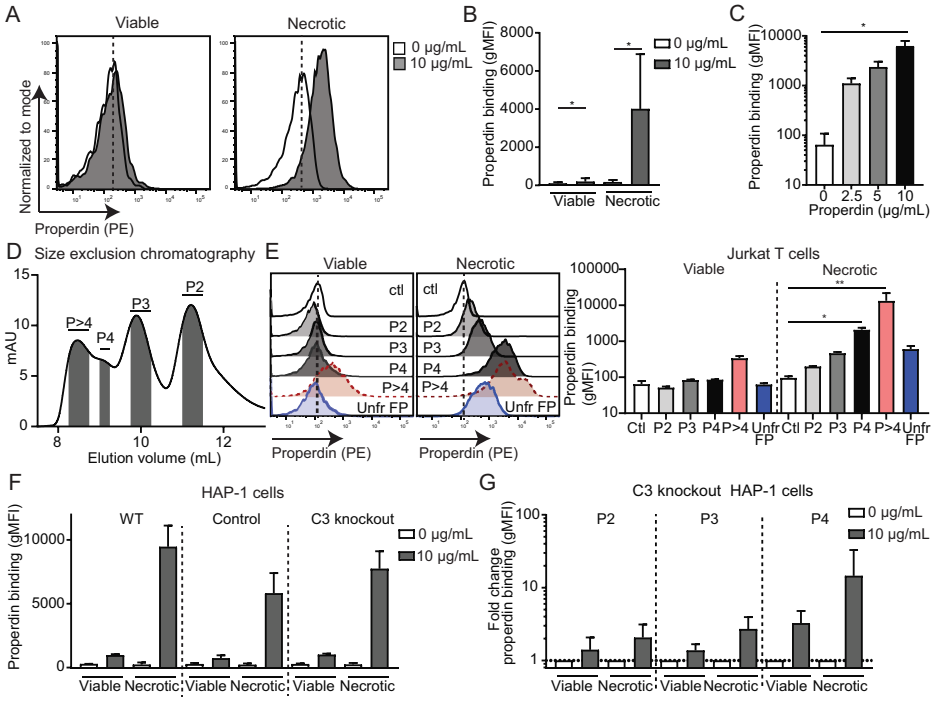

Figure 1: C3-independent properdin binding to necrotic cell surfaces. (A) Representative histograms of the analysis of properdin binding to viable and necrotic Jurkat T cells by flow cytometry after incubation with 10 µg/mL properdin (Quidel). **(B)** Quantification of properdin (10 µg/mL, Quidel) binding to both viable and necrotic Jurkat T cells. Data are presented as mean ± SD of six independent experiments. **(C)** Quantification of properdin binding (0, 2.5, 5 or 10 µg/mL; Quidel) to necrotic Jurkat T cells. Data are presented as mean ± SD of three independent experiments. **(D)** Separation of purified properdin by size exclusion chromatography (SEC) examined in three independent experiments. Fractions were pooled as indicated by the shading in the SEC-profile. Properdin concentration of the pooled fractions were determined by ELISA (P2: 39.3 µg/mL, P3: 41.9 µg/mL, P4: 25.8 µg/mL, P > 4: 14.4 µg/mL). **(E)** Representative histograms of the binding of 10 µg/mL P2, P3, P4, P > 4 and unfractionated properdin (unfr FP) to viable and necrotic Jurkat T cells. Quantification of the data are presented as mean ± SD of the fractions tested on three different viable and necrotic Jurkat T cells batches. The fractions used are a representative for four individual experiments, all showing the interaction of P2, P3 and P4 with necrotic Jurkat T cells. Ctl represent the control conditions of cells incubated with primary and secondary antibodies in the absence of properdin. **(F)** Binding of properdin (10 µg/mL; Quidel) to the surface of viable and necrotic WT HAP-1 cells (WT), CRISPR-Cas9 control cells (control) and a CRISPR-Cas9 derived C3 KO (C3 knockout). Data are presented as mean ± SD of three independent experiments (WT necrotic: mean ± SD of two independent experiments. **(G)** Binding of 10 µg/mL P2, P3 and P4 properdin oligomers, obtained from three independent SEC experiments, to viable and necrotic C3 KO HAP-1 cells. Data are presented as mean ± SD of three independent experiments (for necrotic C3 KO HAP-1 cells) or four independent experiments (for viable C3 KO HAP-1 cells). One way ANOVA-Friedman test and Dunn's multiple comparison test, *$p \leq 0.05$, **$p \leq 0.01$. Wilcoxon matched-pairs signed rank test, paired, *$p \leq 0.05$.

Properdin binding is a prerequisite for AP activation on necrotic cells

To investigate complement activation at the surface of necrotic cells, we first verified complement activation in RPMI, the medium used in our cell cultures, in an ELISA system. In this system, all three pathways of complement could be efficiently activated in a dose-dependent manner (Supporting information Fig. S2). MgEGTA specifically inhibited the CP and LP, but AP activation was maintained. In contrast, 10 mM EDTA completely prevented complement activation in all three pathways (Figure 2A and Supporting information Fig. S2).

Incubation of necrotic Jurkat T cells with 10% normal human serum (NHS) resulted in complement activation, as measured by the deposition of C3 on the cell surface (Figure 2B). Addition of 10 mM EDTA or MgEGTA completely prevented C3 deposition on necrotic cells, suggesting CP or LP activation in RPMI. Preincubation of necrotic Jurkat T cells with properdin, followed by NHS exposure, resulted in a strong increase of C3 deposition when compared to NHS alone. In this case, C3 deposition was not inhibited by MgEGTA, thereby confirming complement activation through the AP (Figure 2B).

To determine subsequent steps of complement activation, we measured C5b-9 deposition on the surface of cells. Only minor C5b-9 deposition was found after exposure to NHS, but this was significantly increased upon prebinding of properdin (Figure 2C). A total of 10 mM EDTA prevented C5b-9 deposition under all conditions. Again, in the presence of MgEGTA, prebinding of properdin resulted in a strong C5b-9 deposition. Therefore, low level C3 and C5b-9 deposition on necrotic Jurkat T cells is mediated by the activation of the CP or LP. However, for AP activation the initial binding of properdin is a prerequisite, thereby resulting in high levels of C3 and C5b9. Also binding of purified oligomeric forms of properdin contributed to C3 deposition via the AP on the surface of necrotic Jurkat T cells, which was not the case for viable Jurkat T cells (Figure 2D). Similar results were observed for C3 deposition on the surface of C3 KO HAP-1 cells (Figure 2E).

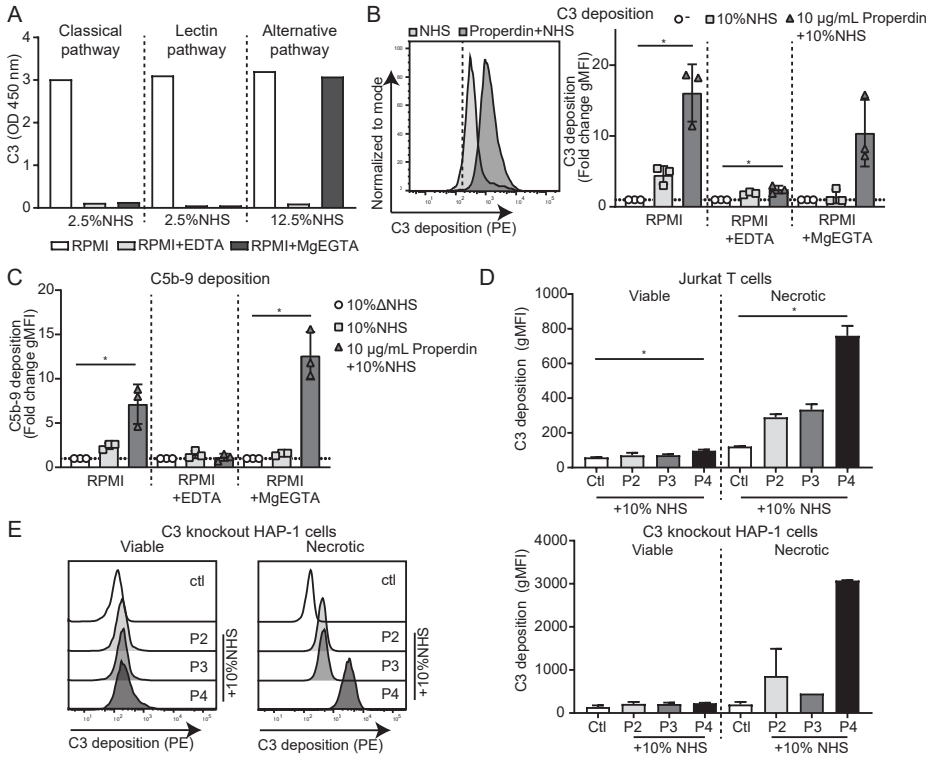

Figure 2: Binding of properdin increases C3 and C5b-9 deposition on necrotic Jurkat T cells. (A) Activation of the complement pathways in RPMI-1640 medium was determined by ELISA. Representative of two independent experiments. **(B)** C3 deposition on necrotic Jurkat T cells in the absence (light grey histograms and bars) or presence (dark grey histograms and bars) of properdin (10 µg/mL, Quidel). Dotted lines in histogram represent the incubation of cells with primary and secondary antibody only. **(C)** C5b-9 deposition on the surface of necrotic Jurkat T cells after exposure to 10% NHS in the absence (light grey bars) or presence of pre-binding of properdin (10 µg/mL, Quidel; dark grey bars). gMFI values were used to calculate the fold change compared to non-exposed (for C3) or 10% ΔNHS exposed (for C5b-9) necrotic Jurkat T cells. Data are presented as the mean ± SD of three independent experiments. **(D)** AP activation on viable and necrotic Jurkat T cells in the absence or presence of 10 µg/mL P2, P3 or P4, determined by C3 deposition. Data are presented as mean ± SD of three independent experiments using P2-P4 fractions from one SEC fractionation. **(E)** AP activation on viable and necrotic C3 knockout HAP-1 cells in the absence or presence of 10 µg/mL P2, P3 or P4, determined by C3 deposition. Data are presented as mean ± SD of two independent experiments (P3 necrotic C3 KO HAP-1: n = 1) using P2-P4 fractions from two different SEC fractionations. One-Way ANOVA-Friedman test and Dunn's multiple comparison test, $*p \leq 0.05$.

Serum components and Salp20 prevent properdin binding, inhibiting AP activation

AP activation on the surface of necrotic Jurkat cells, as shown by C3 (Figure 2B) and C5b-9 (Figure 2C) deposition, was not observed when cells were exposed to NHS, despite properdin being present in this serum. Even with increasing amounts of NHS, up to 50% (containing >10 µg/mL properdin), no binding was observed, whereas incubation with purified properdin did result in binding (Figure 3A). Even more, a dose-

dependent inhibition of properdin binding to necrotic Jurkat T cells was observed when properdin was preincubated with different percentages of ΔNHS (Figure 3B). Inhibition of properdin binding by these serum components also resulted in reduced complement activation on the necrotic cell surface, as determined by C3 deposition (Figure 3C). These results indicate that serum components are able to inhibit initial properdin binding to this cell surface.

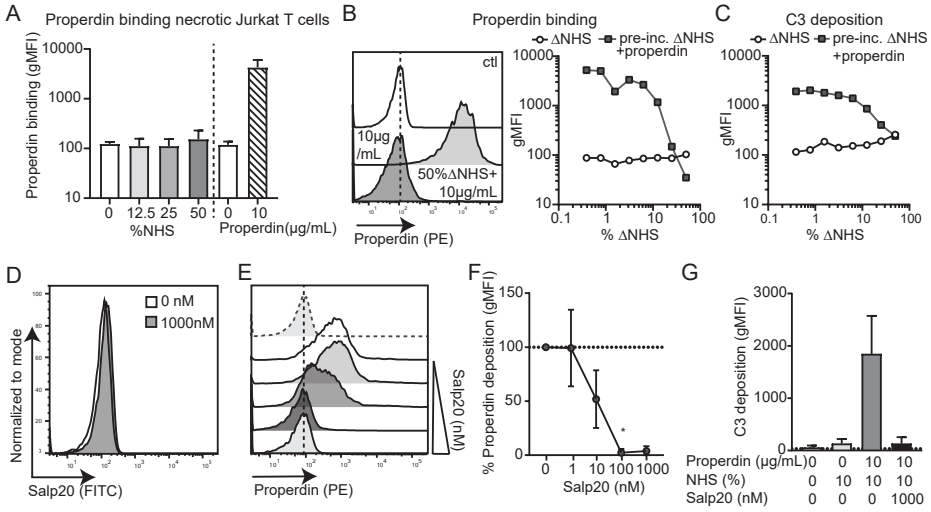

Figure 3: Serum components and Salp20 interfere with properdin binding, disrupting alternative pathway activation. (A) Properdin binding to necrotic Jurkat T cells when incubated with various percentages of NHS or with purified properdin (10 μg/mL, Quidel). Data are presented as the mean ± SD of two independent experiments. **(B)** Properdin (10 μg/mL, Quidel) was preincubated with various percentages of ΔNHS. Effect on properdin binding to necrotic Jurkat T cells was determined using flow cytometry. Ctl in the histogram represents the incubation of cells with primary and secondary antibody only. Representative of two independent experiments. **(C)** Properdin (10 μg/mL, Quidel) was preincubated with various percentages of ΔNHS, followed by incubation with 10% properdin-depleted serum in RPMI-MgEGTA, allowing AP activation. C3 deposition was determined using flow cytometry. Representative of two independent experiments. **(D)** Incubation of necrotic Jurkat T cells with a FITC-labelled Salp20. Representative of two independent experiments. **(E)** Representative histogram of the effect of various concentrations of Salp20 (1,10,100,1000 nM) on properdin (10 μg/mL; Quidel) binding to necrotic Jurkat T cells, analyzed by flow cytometry. **(F)** Quantification of the effect of various Salp20 concentrations on properdin (10 μg/mL, Quidel) binding to necrotic Jurkat T cells. % properdin binding was calculated compared to properdin binding in the absence of Salp20 after background correction. Data are presented as mean ± SD of four independent experiments (1000 nM Salp20: three independent experiments). **(G)** Effect of Salp20 (1000 nM) on AP activation, detected at the level of C3, on necrotic Jurkat T cells. Data are presented as mean ± SD of three independent experiments. One-Way ANOVA-Friedman test and Dunn's multiple comparison test, $*p \leq 0.05$.

To gain further insights into the mechanism of properdin binding to necrotic cells, we used the salivary tick protein Salp20. It has been shown that Salp20 interferes with properdin-C3b interaction and thereby inhibiting the activation of the AP (5, 23,26), but it is unclear whether it interferes with the pattern-recognition function of properdin.

Salp20 did not bind to the surface of necrotic Jurkat T cells directly, as demonstrated using fluorescently-labelled Salp20 (Figure 3D). Salp20 was able to dose-dependently inhibit properdin binding to the surface of necrotic Jurkat T cells when preincubated (Figure 3E and F). Furthermore, Salp20 prevented AP activation on necrotic Jurkat T cells, indicated by the absence of C3 deposition (Figure 3G).

Properdin binds to viable pro- and anti-inflammatory macrophages

Where most complement factors are produced by the liver, properdin is predominantly produced by myeloid cells like DCs and macrophages (19,20). This raises the question whether locally produced properdin can contribute to local complement activation. Properdin was not able to interact with the myeloid cell lines MonoMac6 or U937, unless they were made necrotic (Figure 4A). Therefore, we generated monocyte-derived DCs, proinflammatory macrophages and anti-inflammatory macrophages, and investigated the interaction of properdin with these subpopulations, distinguishing viable and dead cells (Supporting information Fig. S3 and S4A and B). Properdin showed minimal binding to DCs (Figure 4B, mean fold increase 1.3, varying from 0.9- to 1.7-fold). In contrast, a strong binding to the surface of viable proinflammatory macrophages (Figure 4C, mean fold increase 4.3, varying from 1.2- to 15.9-fold) was observed. In all donors tested, a more consistent binding of properdin to anti-inflammatory macrophages was observed (Figure 4D, mean fold increase 3.5, varying from 1.7- to 7.3-fold). In most cases, DCs and pro- and anti-inflammatory macrophages were generated from the same monocyte-population, indicating that the difference in binding is not due to donor variation, but is a result from the differentiation process. The donor variation is also reflected by spread in basal gMFI levels in the absence of exogenous properdin. A similar properdin binding was found upon gating on the small population of dead pro- and anti-inflammatory macrophages (Supporting information Fig. S4A-C).

Activation of the AP on the surface of pro-and anti-inflammatory macrophages, as measured by C3 and C5b-9 deposition, was only observed upon prebinding of properdin and not with NHS alone (Figure 4E-F). Binding of properdin to both macrophage populations could also be demonstrated by the purified oligomers, again showing a more consistent binding to anti-inflammatory macrophages (Figure 4G). Similar results were observed in binding to dead pro-and anti-inflammatory macrophages (Supporting information Fig. S4D). In addition, binding of properdin oligomers contributed to some C3 deposition, especially onto the surface of anti-inflammatory macrophages (Figure 4H). These results show that AP activation can occur at the surface of pro- and anti-inflammatory macrophages, but this depends on initial properdin binding.

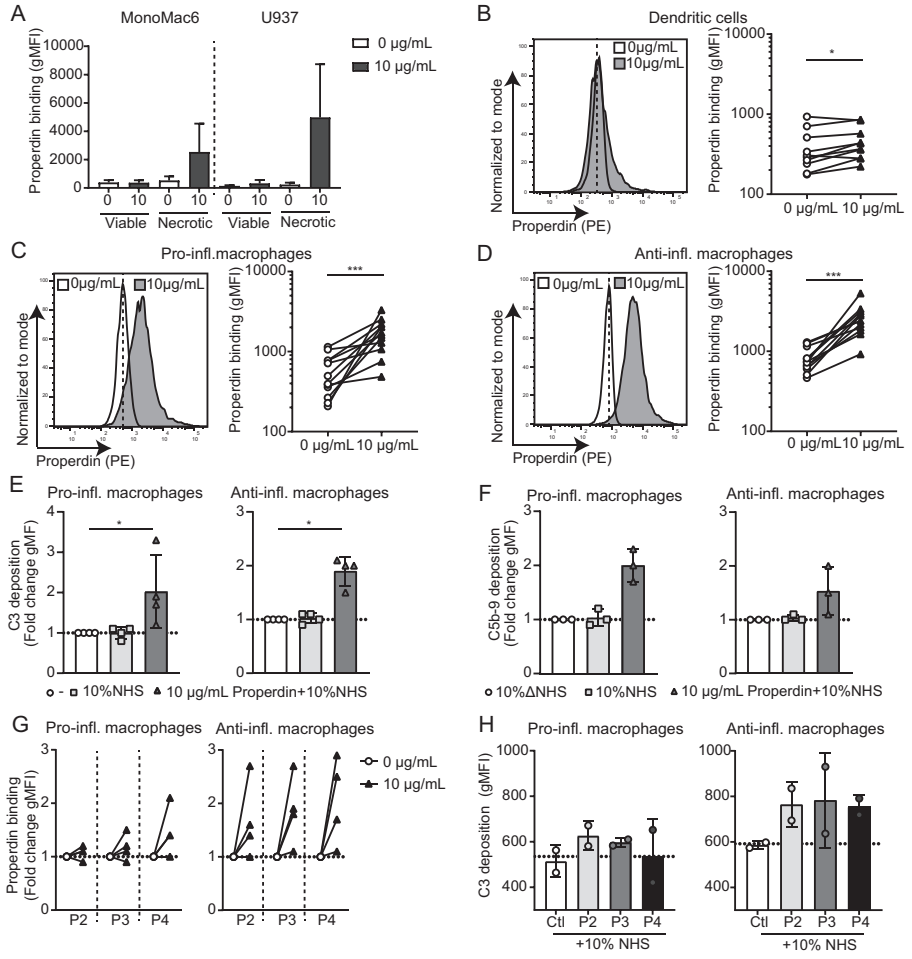

Figure 4: Properdin interacts with the surface of both pro- and anti-inflammatory macrophages, contributing to complement activation. (A) Properdin binding to viable and necrotic monocyte-like cell lines MonoMac6 and U937 analyzed using flow cytometry. Data are presented as mean ± SD of three independent experiments. **(B-D)** Representative histogram and quantification of properdin binding (10 µg/mL; Quidel) to **(B)** DCs (data are obtained from independent experiments performed on DCs generated from 10 different monocyte donors), **(C)** proinflammatory macrophages (data are obtained from independent experiments performed on proinflammatory macrophages generated from 12 different monocyte donors) and **(D)** anti-inflammatory macrophages (data are obtained from independent experiments performed on proinflammatory macrophages generated from 12 different monocyte donors). **(E)** Effect of properdin binding on AP activation on pro- and anti-inflammatory macrophages, determined by C3 deposition. Data are presented as mean ± SD of independent experiments performed on pro- and anti-inflammatory macrophages generated from four different monocyte-donors. **(F)** Effect of properdin binding to pro- and anti-inflammatory macrophages on AP activation measured by C5b-9 deposition. Data are presented as mean ± SD of independent experiments performed on pro- and anti-inflammatory macrophages generated from three different monocyte-donors. **(G)** Proinflammatory macrophages and anti-inflammatory macrophages were incubated with 10 µg/mL P2, P3 and P4 and binding was determined by flow cytometry. Data shown obtained on pro- and anti-inflammatory macrophages generated from four different monocyte donors

(of which two were tested with oligomers from the first SEC, and two with the oligomers from the second SEC). **(H)** Effect of properdin oligomer binding on AP activation on pro- and anti-inflammatory macrophages, determined by C3 deposition. Data are presented as mean ± SD of independent experiments performed on pro- and anti-inflammatory macrophages generated from two different monocyte-donors (incubated with oligomers from the second SEC). Dotted line represent the control condition of cells incubated with primary and secondary antibodies in the absence of properdin and 10%NHS. Wilcoxon matched-pairs signed rank test, paired, *$p \leq 0.05$, ***$p \leq 0.001$. One-Way ANOVA-Friedman test and Dunn's multiple comparison test, *$p \leq 0.05$.

Sulfation pattern and GAG-length are important for properdin binding to cell surfaces

Binding of properdin to viable cells has also been demonstrated for renal proximal tubular epithelial cells, where heparan sulfate was identified as a ligand to which properdin binds (16,17). Therefore, we compared different polysaccharides to determine their inhibitory effect on the binding of properdin to different viable and dead cells. A strong and dose-dependent reduction of binding to necrotic Jurkat T cells as well as viable pro- and anti-inflammatory macrophages was observed when properdin was preincubated with unfractionated heparin (Figure 5A). The results of three independent experiments on necrotic Jurkat T cells, proinflammatory and anti-inflammatory macrophages, using 10 µg/mL of both properdin and the specific polysaccharides, are indicated in a heatmap (Figure 5B, inhibition [blue], increased properdin binding [orange] compared to control [white]). Heparin, but not low-molecular weight heparin, inhibited the binding of properdin to the surface of these cells (Figure 5B, no. 1 vs no. 2). This indicates the importance of the heparin chain length. Fucoidan (no. 8) and dextran sulfate (no. 9) inhibited properdin binding to all cells, whereas heparan sulfate from bovine kidney (no. 7), unsulfated dextran (no. 10), chondroitin sulfate C (no. 11) and chondroitin sulfate B (no. 12) did not (Figure 5B). This indicates that high sulfation is more important than backbone structure for properdin binding to cell surfaces. This was confirmed using *O*-sulfated K5 (no. 5), showing a dose-dependent inhibition of properdin binding for all cell types (Figure 5C). In contrast, unsulfated K5 (no. 6) did not affect properdin binding or in the case of necrotic Jurkat T cells even increased properdin binding (Figure 5C). These results show that binding of properdin to the surfaces of necrotic Jurkat T cells and both pro- and anti-inflammatory macrophages are dependent on GAG charge and length and less on backbone structure.

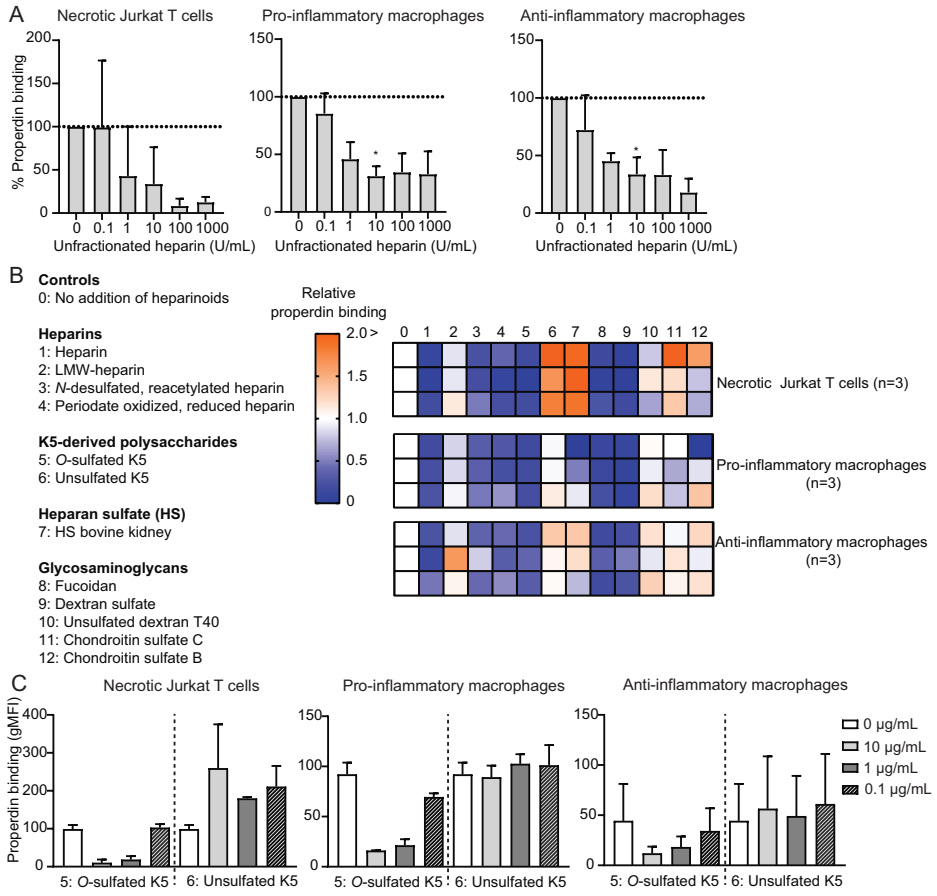

Figure 5: Interaction of properdin with the cell surface of necrotic Jurkat T cells and pro- and anti-inflammatory macrophages depends on glycosaminoglycan charge and length. (A) Quantification of the effect of various concentrations of unfractionated heparin on properdin (10 µg/mL, Quidel) binding to the surface of necrotic Jurkat T cells (left graph), proinflammatory macrophages (middle graph) and anti-inflammatory macrophages (right graph). % properdin binding was calculated compared to properdin binding in the absence of unfractionated heparin (three independent experiments; except for 0.1 and 1000 U/mL, two independent experiments) after background correction. **(B)** Effect of preincubation of properdin (10 µg/mL, Quidel) with various heparins, K5-derived polysaccharides, heparan sulfate, and glycosaminoglycans (10 µg/mL) on properdin binding to the surface of necrotic Jurkat T cells, proinflammatory macrophages and anti-inflammatory macrophages. Data are shown for three independent experiments (pro-and anti-inflammatory macrophages generated from three different monocyte-donors). White squares represents no change in properdin binding, blue squares indicate a lower properdin binding, orange squares indicate an increased properdin binding, all compared to properdin binding without preincubation with heparin-like structures. **(C)** Effect of various concentrations *O*-sulfated K5 and unsulfated K5 (0.1, 1, 10 µg/mL) on properdin (10 µg/mL, Quidel) binding to the surface on necrotic Jurkat T cells (left graph), proinflammatory macrophages (middle graph) and anti-inflammatory macrophages (right graph). Data are presented as mean ± SD of two independent experiments (pro- and anti-inflammatory macrophages were generated from two different monocyte donors). Data are presented as the mean ± SD. One-Way ANOVA-Friedman test and Dunn's multiple comparison test, $*p \leq 0.05$.

Discussion

Properdin is the only known positive regulator of the complement system, able to interact with the AP C3 convertase, thereby stabilizing its half-life five to ten times (2). Recent investigations have shown a potential role for properdin as a PRM, thereby providing a platform for complement activation (9–13). However, in other investigations, properdin was only indicated as a positive regulator of complement activation, completely depended on C3b deposition prior to properdin binding (7,8). Consistent with previous studies (11,28), we demonstrated that properdin is able to bind to the surface of necrotic Jurkat T cells, but also to both viable and necrotic pro- and anti-inflammatory macrophages. It has been suggested that these interactions might be exclusive for nonphysiological aggregates. However, we demonstrate that not only various forms of unfractionated properdin show this activity, but also that binding is observed with fractionated P2, P3 and P4 oligomeric properdin fractions. In addition, we show that properdin binding is a prerequisite for activation of the AP on the cell surfaces. Binding of properdin to the cell surfaces could be inhibited by the salivary tick protein Salp20 and by different polysaccharides, depending on the degree of sulfation and the length of the side chains.

The exact mechanism of how properdin acts as a PRM remains to be elucidated and is still a matter of debate. As discussed in the introduction section, some investigations showed a need of initial C3b deposition prior to binding of properdin (7,8). In addition, it is known that, due to extensive freeze-thaw cycles, nonphysiological forms ("Pn"/P > 4) of properdin can be formed (29). We confirmed the binding of P > 4 to the surface of both viable and necrotic cells. In contrast, physiological forms were only observed to bind necrotic cells, as was also shown in Ref. (28). We only observed binding of purified properdin to necrotic Jurkat T cells, but not to viable Jurkat T cells. In addition, binding of purified properdin was comparable to experiments in which a recombinant form of properdin was used. Fractionation of purified properdin by size exclusion chromatography resulted in a profile as described before (8). These P2-P4 properdin oligomers were able to bind necrotic Jurkat T cells to a similar extend as described in Ref. (28), and binding was not observed to viable Jurkat T cells.

It has been proposed that initial C3b deposition is required, prior to binding of properdin (7,8). We have investigated the C3-dependence of properdin binding using C3 KO HAP-1 cells. We have confirmed that properdin was able to bind to the surface of C3-deficient cells, to a similar extent as to WT and CRISPR-Cas9 control cells. Similar results were previously observed for properdin binding to necrotic $C3^{-/-}$ mice splenocytes (11) and recently, properdin binding to the bacterial surface of *Leptospira* was described to occur

in the absence of C3b (30). Furthermore, our group showed the deposition of properdin in the glomeruli of C3 KO mice with induced acute antiglomerular basement membrane disease, showing C3b-independent properdin binding (14). In addition, it was recently described that P4 was able to bind to soluble collectin-12 opsonized bacteria *Aspergillus fumigatus* in a C3-independent manner (31). Altogether, we conclude that properdin is able to interact with various cells or cell surfaces in the absence of C3.

Research in which properdin binding was shown to be C3b-dependent was performed in serum, and therefore properdin was surrounded by multiple serum components (7). In contrast, direct properdin binding to zymosan or chlamydia could be observed using purified properdin, but in both cases was reported to be inhibited by human serum (28,32). In line with previous results (28), we now confirm that human serum also dose-dependently inhibits the binding of purified properdin to necrotic cells and prevents subsequent alternative pathway activation (Figure 3 B-C). It has been suggested that pentraxin serum amyloid P (33) and monomeric C-reactive protein (34) might be partially responsible for this inhibition, but characterization of the inhibitory factor(s) needs further validation. Nevertheless, these results further underline the importance of myeloid cells as the source of properdin production. Local production of properdin in tissues and at sites of inflammation, in the absence of other serum components, will facilitate that properdin can act as a PRM.

An intriguing question is why such an important mechanism as the initiation of the alternative pathway of complement activation would depend on spontaneous hydrolysis of C3, combined with a random deposition. It has been demonstrated that properdin can interact with low affinity with the CTC domain present in intact C3/C3b (SPR experiments; K_D= 19 ± 2 μM) (5), which would be feasible in view of the high C3 concentrations in serum. Therefore, opsonization of different surfaces with properdin would provide a mechanism how the hydrolysis of C3 could preferentially occur in the close vicinity of these targeted surfaces. We recently confirmed that in a cell mixture, properdin selectively directs complement activation onto the cell surface to which properdin is bound. Upon exposure to NHS in the presence of MgEGTA, only allowing activation of the AP, C3 deposition was predominantly found on these properdin-opsonized cells (data not shown).

Properdin is able to bind to proximal tubular epithelial cells and it has been shown that heparan sulfates are involved in this interaction (12,16,17). We also investigated the properdin binding to viable DCs and macrophages and observed a properdin binding to both pro- and anti-inflammatory macrophages (Figure 4), partially confirming data of properdin binding to anti-inflammatory macrophages (10). DCs and macrophages

express various proteo- and GAGs at the cell surface (35,36). The less efficient properdin binding to DCs, and the absence of interaction with the myeloid cell lines MonoMac6 and U937, might be explained by a distinct surface composition. However, further research is needed to identify the molecular differences. We investigated which proteoglycans were able to compete with the binding of properdin to the investigated cell surfaces. To reduce the risk of losing proteoglycan structures on these cell surfaces, cells were not harvested by trypsin digestion, instead a non-enzymatic solution was used. Reduced properdin binding to the cellular surface was observed with (unfractionated) heparin. The length of the heparin chain seems to be important, since low molecular weight heparin did not inhibit properdin binding to the cell surface. The degree of sulfate groups on GAGs seemed also important, since *O*-sulfated K5 was able to inhibit properdin binding, whereas unsulfated K5 was not. Furthermore, dextran sulfate is able to reduce properdin binding to the cell surface, whereas unsulfated dextran is not (Figure 5). These findings correspond with previous findings, highlighting the importance of certain GAGs in facilitating properdin binding (16). The binding of properdin with GAGs is likely mediated through electrostatic interactions as properdin is highly positive and is known to interact with negatively charged ligands (e.g., GAGs and DNA) (11). Factor H is also able to interact with the cell surface via proteoglycans, contributing to local regulation of complement activation (37,38).

The binding of properdin to necrotic Jurkat T cells might affect phagocytosis. Binding of properdin enhances complement activation, thereby increasing local C3b levels. C3b opsonized cells can be detected by complement receptors expressed on phagocytes, resulting in removal of the dead cells (39,40). We observed binding of properdin to the surface of both necrotic cells and macrophages. Properdin-bound necrotic cells could therefore interact with macrophages, suggesting a role in phagocytosis. Such a potential role of properdin in facilitating the bridging of cells was discussed recently, and would likely require higher oligomeric properdin structures like P3 and P4, allowing binding to both surfaces via unoccupied binding sites (41). Alternatively, specific properdin receptors, like NKp46, could play a role in these processes. NKp46 is expressed on innate lymphoid cells like NK cells and is able to bind properdin (42). It was shown that this interaction was required for the survival of mice infected with *Neisseria meningitidis* (42). However, in the context of the current research its contribution would be less likely, since NKp46 receptor expression is not describe on macrophages.

Altogether, our findings show that purified properdin and P2, P3 and P4 oligomers are able to bind to the surface of necrotic Jurkat T cells and pro- and anti-inflammatory macrophages, whereas only the nonphysiological form of properdin (P > 4) is able to bind to the surface of viable Jurkat T cells. The binding of properdin contributes to local

complement activation. This work provides a foundation for further research about the role of locally produced properdin and its binding to the surface of these cells.

Acknowledgments

We thank Prof. R.C. Hoeben for his help in the generation of C3-deficient HAP-1 cells. The HAP-1 cell line used for the CRISPR-Cas9 experiments was a kind gift from R. Spaapen, Sanquin Research, Amsterdam, The Netherlands. The COMBAT consortium is sponsored by the Dutch Kidney Foundation (grant 13OCA27). The COMBAT consortium is an inter-university collaboration in the Netherlands that is formed to study basic mechanisms, assay development and therapeutic translation of complement-mediated renal diseases. Principal investigators are (in alphabetical order): S. Berger (Department of Internal Medicine-Nephrology, University Medical Center Groningen, The Netherlands), J. van den Born (Department of Internal Medicine-Nephrology, University Medical Center Groningen, The Netherlands), P. Gros (Department of Chemistry, Utrecht University, The Netherlands), L. van den Heuvel (Department of Pediatric Nephrology, Radboud University Medical Center, Nijmegen, The Netherlands), N. van de Kar (Department of Pediatric Nephrology, Radboud University Medical Center, Nijmegen, The Netherlands), C. van Kooten (Department of Internal Medicine-Nephrology, Leiden University Medical Center, The Netherlands), M. Seelen (Department of Internal Medicine-Nephrology, University Medical Center Groningen, The Netherlands), A. de Vries (Department of Internal Medicine-Nephrology, Leiden University Medical Center, The Netherlands).

References

1. Walport MJ. Complement. First of two parts. N Engl J Med. 2001 Apr 5;344(14):1058-66. doi: 10.1056/NEJM200104053441406.
2. Fearon DT, Austen KF. Properdin: binding to C3b and stabilization of the C3b-dependent C3 convertase. J Exp Med. 1975 Oct 1;142(4):856-63. doi: 10.1084/jem.142.4.856.
3. Smith CA, Pangburn MK, Vogel CW, Müller-Eberhard HJ. Molecular architecture of human properdin, a positive regulator of the alternative pathway of complement. J Biol Chem. 1984 Apr 10;259(7):4582-8.
4. Pedersen DV, Gadeberg TAF, Thomas C, Wang Y, Joram N, Jensen RK, et al. Structural basis for properdin oligomerization and convertase stimulation in the human complement system. Front Immunol. 2019 Aug 22;10:2007. doi: 10.3389/fimmu.2019.02007.
5. van den Bos RM, Pearce NM, Granneman J, Brondijk THC, Gros P. Insights into enhanced complement activation by structures of properdin and its complex with the C-terminal domain of C3b. Front Immunol. 2019 Sep 4;10:2097. doi: 10.3389/fimmu.2019.02097.
6. Kemper C, Atkinson JP, Hourcade DE. Properdin: emerging roles of a pattern-recognition molecule. Annu Rev Immunol. 2010;28:131-55. doi: 10.1146/annurev-immunol-030409-101250.
7. Harboe M, Garred P, Lindstad JK, Pharo A, Müller F, Stahl GL, et al. The role of properdin in zymosan- and Escherichia coli-induced complement activation. J Immunol. 2012 Sep 1;189(5):2606-13. doi: 10.4049/jimmunol.1200269.
8. Harboe M, Johnson C, Nymo S, Ekholt K, Schjalm C, Lindstad JK, et al. Properdin binding to complement activating surfaces depends on initial C3b deposition. Proc Natl Acad Sci U S A. 2017 Jan 24;114(4):E534-E539. doi: 10.1073/pnas.1612385114.
9. Spitzer D, Mitchell LM, Atkinson JP, Hourcade DE. Properdin can initiate complement activation by binding specific target surfaces and providing a platform for de novo convertase assembly. J Immunol. 2007 Aug 15;179(4):2600-8. doi: 10.4049/jimmunol.179.4.2600.
10. Kemper C, Mitchell LM, Zhang L, Hourcade DE. The complement protein properdin binds apoptotic T cells and promotes complement activation and phagocytosis. Proc Natl Acad Sci U S A. 2008 Jul 1;105(26):9023-8. doi: 10.1073/pnas.0801015105.
11. Xu W, Berger SP, Trouw LA, de Boer HC, Schlagwein N, Mutsaers C, et al. Properdin binds to late apoptotic and necrotic cells independently of C3b and regulates alternative pathway complement activation. J Immunol. 2008 Jun 1;180(11):7613-21. doi: 10.4049/jimmunol.180.11.7613.
12. Gaarkeuken H, Siezenga MA, Zuidwijk K, van Kooten C, Rabelink TJ, Daha MR, et al. Complement activation by tubular cells is mediated by properdin binding. Am J Physiol Renal Physiol. 2008 Nov;295(5):F1397-403. doi: 10.1152/ajprenal.90313.2008.
13. Kemper C, Hourcade DE. Properdin: New roles in pattern recognition and target clearance. Mol Immunol. 2008 Oct;45(16):4048-56. doi: 10.1016/j.molimm.2008.06.034.
14. O'Flynn J, Kotimaa J, Faber-Krol R, Koekkoek K, Klar-Mohamad N, Koudijs A, et al. Properdin binds independent of complement activation in an in vivo model of anti-glomerular basement membrane disease. Kidney Int. 2018 Dec;94(6):1141-1150. doi: 10.1016/j.kint.2018.06.030.

15. Zaferani A, Vivès RR, van der Pol P, Navis GJ, Daha MR, van Kooten C, et al. Factor h and properdin recognize different epitopes on renal tubular epithelial heparan sulfate. J Biol Chem. 2012 Sep 7;287(37):31471-81. doi: 10.1074/jbc.M112.380386.

16. Zaferani A, Vivès RR, van der Pol P, Hakvoort JJ, Navis GJ, van Goor H, et al. Identification of tubular heparan sulfate as a docking platform for the alternative complement component properdin in proteinuric renal disease. J Biol Chem. 2011 Feb 18;286(7):5359-67. doi: 10.1074/jbc.M110.167825.

17. Lammerts RGM, Talsma DT, Dam WA, Daha MR, Seelen MAJ, Berger SP, et al. Properdin pattern recognition on proximal tubular cells is heparan sulfate/syndecan-1 but not C3b dependent and can be blocked by tick protein Salp20. Front Immunol. 2020 Aug 7;11:1643. doi: 10.3389/fimmu.2020.01643.

18. Wirthmueller U, Dewald B, Thelen M, Schäfer MK, Stover C, Whaley K, et al. Properdin, a positive regulator of complement activation, is released from secondary granules of stimulated peripheral blood neutrophils. J Immunol. 1997 May 1;158(9):4444-51.

19. Dixon KO, O'Flynn J, Klar-Mohamad N, Daha MR, van Kooten C. Properdin and factor H production by human dendritic cells modulates their T-cell stimulatory capacity and is regulated by IFN-γ. Eur J Immunol. 2017 Mar;47(3):470-480. doi: 10.1002/eji.201646703.

20. Cortes C, Ohtola JA, Saggu G, Ferreira VP. Local release of properdin in the cellular microenvironment: role in pattern recognition and amplification of the alternative pathway of complement. Front Immunol. 2013 Jan 17;3:412. doi: 10.3389/fimmu.2012.00412.

21. Li K, Fazekasova H, Wang N, Sagoo P, Peng Q, Khamri W, et al. Expression of complement components, receptors and regulators by human dendritic cells. Mol Immunol. 2011 May;48(9-10):1121-7. doi: 10.1016/j.molimm.2011.02.003.

22. Lubbers R, van Essen MF, van Kooten C, Trouw LA. Production of complement components by cells of the immune system. Clin Exp Immunol. 2017 May;188(2):183-194. doi: 10.1111/cei.12952.

23. Tyson KR, Elkins C, de Silva AM. A novel mechanism of complement inhibition unmasked by a tick salivary protein that binds to properdin. J Immunol. 2008 Mar 15;180(6):3964-8. doi: 10.4049/jimmunol.180.6.3964.

24. Hourcade DE, Akk AM, Mitchell LM, Zhou HF, Hauhart R, Pham CT. Anti-complement activity of the Ixodes scapularis salivary protein Salp20. Mol Immunol. 2016 Jan;69:62-9. doi: 10.1016/j.molimm.2015.11.008.

25. van Essen MF, Schlagwein N, van Gijlswijk-Janssen DJ, Anholts JDH, Eikmans M, Ruben JM, et al. Culture medium used during small interfering RNA (siRNA) transfection determines the maturation status of dendritic cells. J Immunol Methods. 2020 Apr;479:112748. doi: 10.1016/j.jim.2020.112748.

26. Michels MAHM, van de Kar NCAJ, van den Bos RM, van der Velden TJAM, van Kraaij SAW, Sarlea SA, et al. Novel assays to distinguish between properdin-dependent and properdin-independent C3 nephritic factors provide insight into properdin-inhibiting therapy. Front Immunol. 2019 Jun 17;10:1350. doi: 10.3389/fimmu.2019.01350.

27. Cossarizza A, Chang HD, Radbruch A, Acs A, Adam D, Adam-Klages S, et al. Guidelines for the use of flow cytometry and cell sorting in immunological studies (second edition). Eur J Immunol. 2019 Oct;49(10):1457-1973. doi: 10.1002/eji.201970107.

28. Ferreira VP, Cortes C, Pangburn MK. Native polymeric forms of properdin selectively bind to targets and promote activation of the alternative pathway of complement. Immunobiology. 2010 Nov;215(11):932-40. doi: 10.1016/j.imbio.2010.02.002.

29. Farries TC, Finch JT, Lachmann PJ, Harrison RA. Resolution and analysis of 'native' and 'activated' properdin. Biochem J. 1987 Apr 15;243(2):507-17. doi: 10.1042/bj2430507.

30. Martinez APG, Abreu PAE, de Arruda Vasconcellos S, Ho PL, Ferreira VP, Saggu G, et al. The role of properdin in killing of non-pathogenic Leptospira biflexa. Front Immunol. 2020 Nov 10;11:572562. doi: 10.3389/fimmu.2020.572562.

31. Zhang J, Song L, Pedersen DV, Li A, Lambris JD, Andersen GR, et al. Soluble collectin-12 mediates C3-independent docking of properdin that activates the alternative pathway of complement. Elife. 2020 Sep 10;9:e60908. doi: 10.7554/eLife.60908.

32. Cortes C, Ferreira VP, Pangburn MK. Native properdin binds to Chlamydia pneumoniae and promotes complement activation. Infect Immun. 2011 Feb;79(2):724-31. doi: 10.1128/IAI.00980-10.

33. Mitchell L, Hourcade D. Inhibition of properdin-directed complement activation by serum amyloid P component. Mol Immunol. 2008 Oct; 45(16):4103–4. https://doi.org/10.1016/j.molimm.2008.08.026

34. O'Flynn J, van der Pol P, Dixon KO, Prohászka Z, Daha MR, van Kooten C. Monomeric C-reactive protein inhibits renal cell-directed complement activation mediated by properdin. Am J Physiol Renal Physiol. 2016 Jun 1;310(11):F1308-16. doi: 10.1152/ajprenal.00645.2014.

35. Wegrowski Y, Milard AL, Kotlarz G, Toulmonde E, Maquart FX, Bernard J. Cell surface proteoglycan expression during maturation of human monocytes-derived dendritic cells and macrophages. Clin Exp Immunol. 2006 Jun;144(3):485-93. doi: 10.1111/j.1365-2249.2006.03059.x.

36. Hatano S, Watanabe H. Regulation of macrophage and dendritic cell function by chondroitin sulfate in innate to antigen-specific adaptive immunity. Front Immunol. 2020 Mar 3;11:232. doi: 10.3389/fimmu.2020.00232.

37. Józsi M, Zipfel PF. Factor H family proteins and human diseases. Trends Immunol. 2008 Aug;29(8):380-7. doi: 10.1016/j.it.2008.04.008.

38. Langford-Smith A, Day AJ, Bishop PN, Clark SJ. Complementing the sugar code: role of GAGs and sialic acid in complement regulation. Front Immunol. 2015 Feb 2;6:25. doi: 10.3389/fimmu.2015.00025.

39. Martin M, Blom AM. Complement in removal of the dead - balancing inflammation. Immunol Rev. 2016 Nov;274(1):218-232. doi: 10.1111/imr.12462.

40. Westman J, Grinstein S, Marques PE. Phagocytosis of necrotic debris at sites of injury and inflammation. Front Immunol. 2020 Jan 9;10:3030. doi: 10.3389/fimmu.2019.03030.

41. Pedersen DV, Pedersen MN, Mazarakis SM, Wang Y, Lindorff-Larsen K, Arleth L, et al. Properdin oligomers adopt rigid extended conformations supporting function. Elife. 2021 Jan 22;10:e63356. doi: 10.7554/eLife.63356.

42. Narni-Mancinelli E, Gauthier L, Baratin M, Guia S, Fenis A, Deghmane AE, et al. Complement factor P is a ligand for the natural killer cell-activating receptor NKp46. Sci Immunol. 2017 Apr 28;2(10):eaam9628. doi: 10.1126/sciimmunol.aam9628.

Supporting information

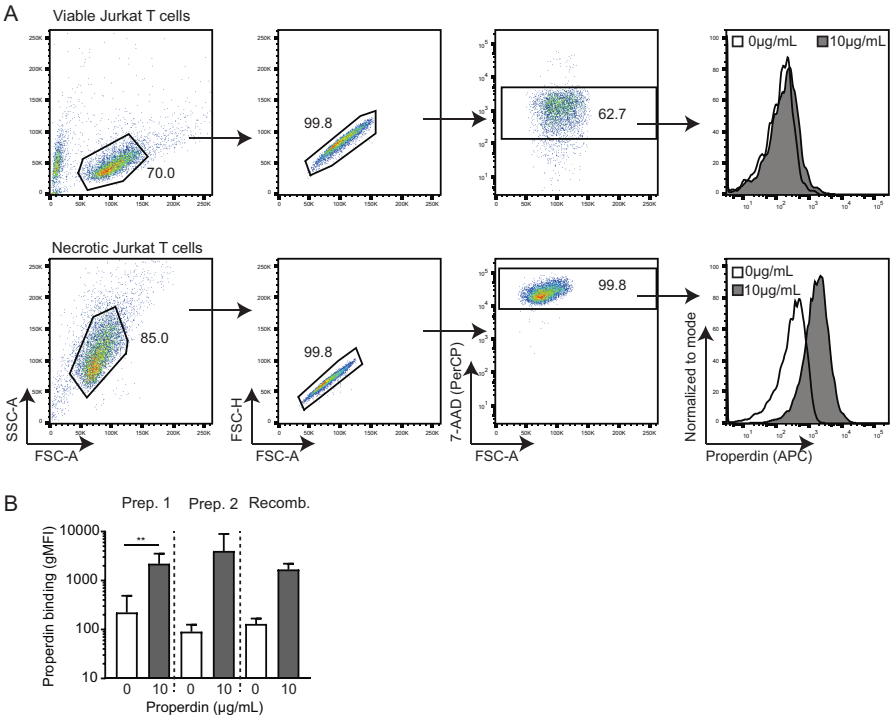

Fig. S1: Discrimination of viable and necrotic Jurkat T cells. (A) Jurkat T cells were made necrotic by resuspending the cells in RPMI-1640 (no phenol red, 11835-063, Gibco/Life technologies) and incubate them for 30 minutes at 56˚C. Cell death was confirmed by microscopy (using Trypan Blue stain, cat 17-942E, BioWhittaker, Walersville, MD, USA), and by flow cytometry using 7-AAD (PerCP, 1:25, 559925, BD). Cells were gated based on FSC-A vs SSC-A, followed by the selection of single cells (FSC-A vs FSC-H). Discrimination between viable (7-AAD-) and necrotic Jurkat T cells (7-AAD+) was made. Properdin binding to the viable and necrotic cells was examined on an histogram. Numbers indicate the percentages of cells present in the gates. In other experiments, viable and necrotic cells were gated based on FSC-A vs SSC-A. **(B)** Quantification of properdin binding from various preparations to necrotic Jurkat T cells. Properdin from either Quidel (Prep . 1), CompTech (Prep. 2) or a recombinant form of properdin (Recomb.) were used (mean±SD of 9 (Quidel), 3 (CompTech) and 2 (Recomb.) independent experiments. Wilcoxon matched-pairs signed rank test, **P≤.01.

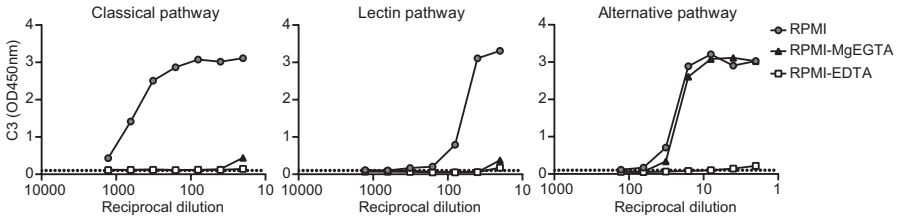

Fig. S2: Activation of complement pathways in RPMI-1640 medium. Classical pathway (CP), lectin pathway (LP) and alternative pathway (AP) activity in normal human serum (NHS) was determined by ELISA. In brief, to determine CP activity, human IgM (3 µg/mL, isolated in-house) was coated in coating buffer (0.1 M NaHCO3, 0.1 M Na2CO3, pH 9.6) overnight at room temperature. For LP activation, mannan (from *Saccharomyces cerevisiae*, 10 µg/mL, M7504-1G, Sigma-Aldrich, Saint Louis, MO, USA) was coated in coating buffer overnight at room temperature and for AP activation, plates were coated with LPS (*S. Enteritidis*, 10 µg/mL, HC4069, Hycult Biotech, Uden, The Netherlands) in 10mM MgCl2 in PBS, overnight at room temperature. Plates were blocked for 1hr at 37°C. To determine complement activation in the medium, NHS was diluted in RPMI-1640 (no phenol red) which should allow activation of all complement pathways. Inhibition of the pathways was investigated by diluting NHS in RPMI-EDTA (RPMI-1640 supplemented by 10mM EDTA). Activation of only the AP was investigated by NHS dilution in RPMI-MgEGTA (RPMI containing 10mM EGTA and 5mM MgCl2). For CP/LP activity, NHS was analysed in reciprocal 1.5-fold dilutions starting from 5%. For AP activity, NHS was analysed in reciprocal 1.5-fold dilutions starting from 20%. Diluted serum samples were incubated for 1hr at 37°C. Next, plates were washed with washing buffer (PBS with 0.05% Tween-20 (Sigma-Aldrich)) and C3 deposition was determined by incubation with RFK22 (digoxigenin (DIG) labelled, in house generated, 1/10.000; dilution of antibodies in PBS with 0.05%Tween20 and 1%BSA) for 1hr at 37°C. Plates were washed and incubated for 1hr at 37°C to determine the deposition using peroxidase-conjugated IgG fraction monoclonal mouse anti-DIG (0.1 µg/mL, 200-032-156, Jackson ImmunoResearch, Cambridgeshire, UK). Plates were washed and developed using TMB. Dotted lines in graphs indicate the background in the assay. Representative of 2 independent experiments.

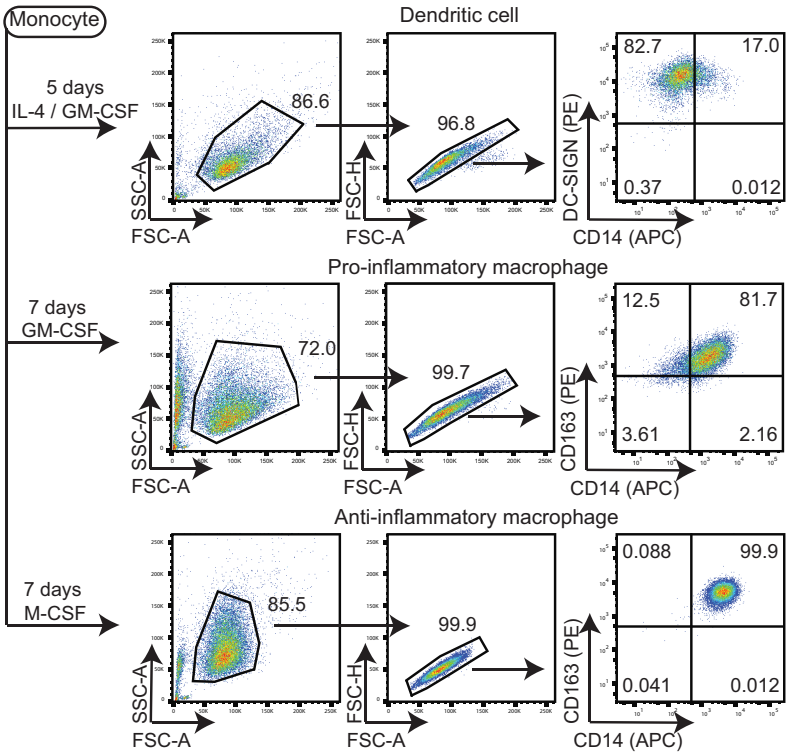

Fig. S3: Generation of monocyte-derived dendritic cells, proinflammatory and anti-inflammatory macrophages. Generation of dendritic cells by culturing isolated monocytes for 5 days with IL-4 and GM-CSF. Differentiation was examined by mouse-anti-human DC-SIGN (PE, 1:50, CD209, Clone 9E9A8, 330106, Biolegend) and mouse anti-human CD14 (APC, 1:200, Clone MφP9, cat no. 345787, BD). Pro- and anti-inflammatory macrophages were generated by incubating isolated monocytes with GM-CSF or M-CSF for 7 days, respectively. Differentiation was examined by flow cytometry using mouse-anti human CD163 (PE, 1:20, Clone GHI/61, 333606, Biolegend) and mouse anti-human CD14. For all donors, dendritic cell and macrophage differentiation was examined. Viable cells were gated based on FSC-A vs SSC-A, and in this example single cells were selected based on FSC-A vs FSC-H.

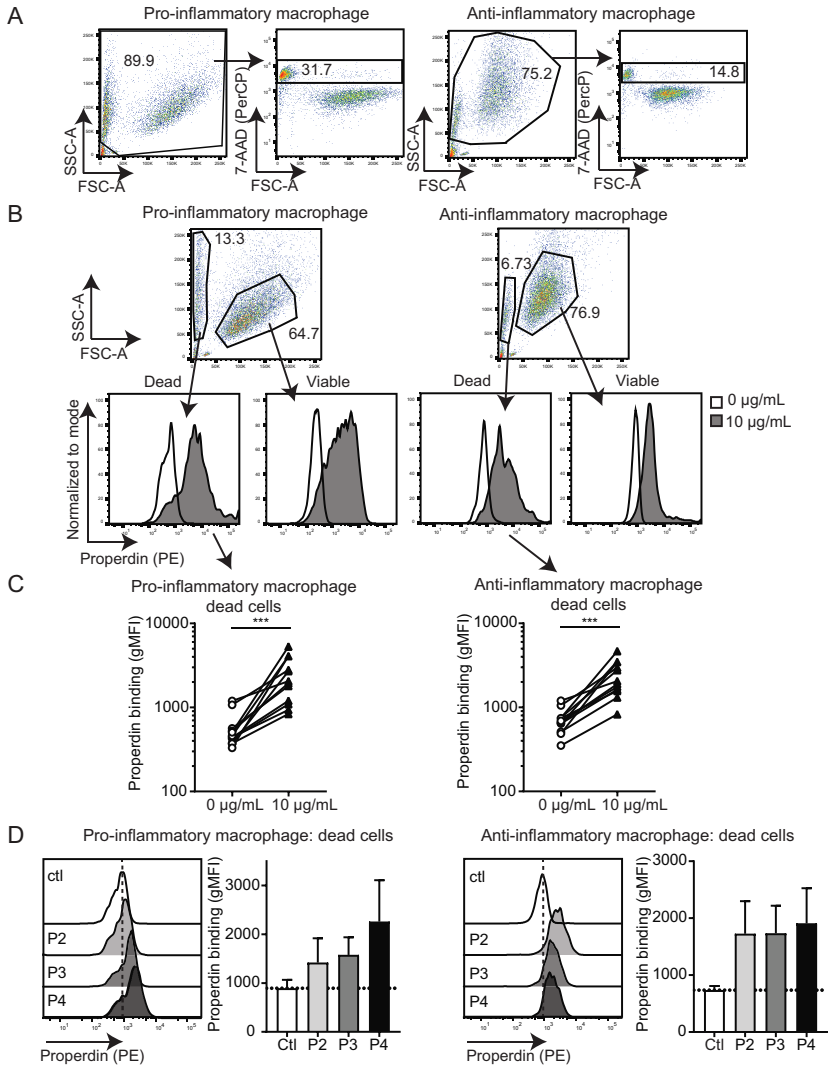

Fig. S4: Properdin binding to the surface of dead macrophages. (A) Discrimination between viable and dead pro-and anti-inflammatory macrophages by analysing 7-AAD-positivity by flow cytometry. **(B)** FSC-A vs SSC-A selection of both dead and viable pro-and anti-inflammatory macrophages, followed by the examination of properdin binding to these populations on a histogram. **(C)** Quantification of properdin binding to the surface of dead pro- and anti-inflammatory macrophages. Data are obtained from independent experiments performed on pro-and anti-inflammatory macrophages generated from 12 different monocyte donors. **(D)** Examination of the binding of properdin oligomers P2, P3 and P4 to dead pro- and anti-inflammatory macrophages by flow cytometry. Data are presented as mean±SD of 4 biological replicates on dead pro- and anti-inflammatory macrophages (generated from 4 different monocyte donors, of which 2 were tested with oligomers from the first SEC, and 2 with the oligomers from the second SEC). Wilcoxon matched pairs signed rank test, ***P≤.001.